DOI: 10.1002/chem.200601490

The Low-Barrier Hydrogen Bond of Deuterated Benzoylacetone Probed by Very Low Temperature Neutron and X-ray Diffraction Studies and Theoretical Calculations

Georg K. H. Madsen,*[a] Garry J. McIntyre,[b] Birgit Schiøtt,[a] and Finn K. Larsen[a]

Abstract: Low-temperature neutron diffraction data is used to show that the enol deuteron in deuterated benzoylacetone has a bimodal probability density distribution. In a previous study of normal benzoylacetone we showed that the enol hydrogen atom has a broad unimodal probability density distribution. Deuteration gives hardly any change to the molecular framework other than a small lengthening of the O···O distance. We solve the vibrational Hamiltonian for a series of model hydrogen potentials and show how the proton/deuteron probability density function can become strongly perturbed by small changes to the potential. The potentials are used to show that the deuteron in benzoylacetone can be interpreted as an atom tunnelling between two possible localised positions, while the proton in benzoylacetone can be viewed as having sufficient energy to shuttle over the low-energy barrier, even at 15 K. We underline the necessity of accounting for the dynamic nature of the hydrogen bond and not relying on a description of the proton/deuteron by a single atomic coordinate, and compare our results to structure correlation studies.

Keywords: deuterium · enzyme catalysis · hydrogen bonds · low-barrier tunneling · neutron diffraction

Introduction

Hydrogen bonds (HB) have received much attention due to their fundamental interest and to their importance in molecular recognition processes.[1–3] They can be classified into three categories,[2] for example in the case of O–H···O HBs: 1) Weak with O···O distances above 3.2 Å, 2) moderately strong (normal) with distances ranging from approximately 2.5 to 3.2 Å and 3) strong with distances shorter than 2.5 Å. Based on the nature of the potential well in which the hydrogen resides, strong HBs have been further subdivided[1] into strong HBs and very strong HBs. In the strong HB the zero-point vibrational energy (ZPVE) of the hydrogen (but not of deuterium) atom exceeds the proton-transfer barrier. These strong HBs have also been named low-barrier hydrogen bonds (LBHB).[4] In the very strong HBs both hydrogen and deuterium atoms have sufficient ZPVE to shuttle between the two hydrogen-bonded acceptors.

It has been inferred from spectroscopic evidence,[1] crystal correlation methods[5] and studies of the electron density[6,7] that short hydrogen bonds have a strong covalent contribution. This covalent contribution can be expected to be important for the large HB energies up to 160 kJ mol^{-1} found for short hydrogen bonds.[2] Because of this large gain in energy strong hydrogen bonds have been postulated to play an important role in enzyme catalysis.[8] However, the existence and importance of strong hydrogen bonds in enzyme catalysis is a controversial theme.[9–11]

Anharmonic motion and quantum effects such as zero-point motion and tunnelling are important for the hydrogen dynamics. This makes a full treatment by ab initio calculations very difficult. Such effects have been included by using Feynman path integral techniques, providing very detailed information about the proton dynamics. One very illustrative example is the study of the high-pressure phase of ice.[12] The time-averaged proton distribution function was studied and it was demonstrated that as the water molecules are forced closer, the hydrogen atom goes from being located at one oxygen atom to tunnelling between two oxygen atoms to finally, at high pressures, being located midway between two oxygen atoms.[12]

[a] Dr. G. K. H. Madsen, Dr. B. Schiøtt, Dr. F. K. Larsen
Department of Chemistry, University of Aarhus
8000 Århus C (Denmark)
Fax: (+45) 8619-6199
E-mail: georg@chem.au.dk

[b] Dr. G. J. McIntyre
Institut Laue-Langevin, BP 156
38042 Grenoble Cedex 9 (France)

Recently a lot of attention has been given to the so-called migrating proton that can be found in both O–H···O[13–15] and N–H···O systems.[16–18] The structural consequences of deuterating the short hydrogen bond have been studied less, although considerable consequences for the lower ZPVE of a deuteron in a strong HB can be envisaged. If the HB has a low-barrier but the energy difference between the two minima is sufficiently asymmetric, a hydrogen atom could exhibit significant motion between the atoms, while a deuteron would fall out on one side. To our knowledge such a situation has only been observed once.[19,20] These neutron diffraction studies of the short HB bridging the ligands in a Ni complex, bis(2-amino-2-methyl-3-butanone oximato)nickel(II) chloride monohydrate (Ni–AMBO), offer one convincing example of a structural change upon deuteration. The hydrogen atom was located in a broad, slightly asymmetric potential well for the normal complex,[19] while in the deuterated complex the deuterium atom resided in a narrow and much more asymmetric potential well.[20] The results for the Ni complex can be interpreted as a proton in a LBHB with a large enough energy difference between the possible deuteron positions for it to become localised. However, if the energy difference between the two positions is sufficiently small, the deuteron may tunnel between the two positions. To our knowledge a direct observation by neutron scattering of such a situation has not been reported previously, but we have now observed this to take place in deuterated benzoylacetone (DBA).

Previously we reported a very low temperature combined neutron and X-ray diffraction study of hydrogenated benzoylacetone (HBA).[6] We demonstrated that the structure is ordered with the enol hydrogen atom located close to the midpoint between the two oxygen atoms, but with a very large mean-square displacement (MSD) along the O···O vector. The large MSD was interpreted as the hydrogen atom having a sufficiently large ZPVE to vibrate freely between the two oxygen atoms.[6] The present paper describes the change of structure which occurs upon deuteration of the enol position.

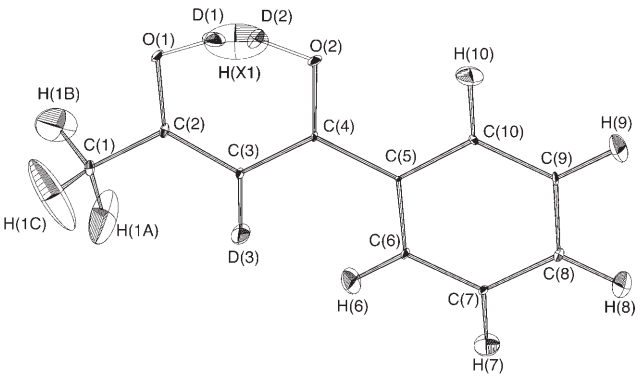

Figure 1. ORTEP drawing of the deuterated benzoylacetone molecule showing the 50% probability ellipsoids obtained by refinement of the neutron data. For comparison a thermal ellipsoid with the positional and thermal parameters obtained from HBA[6] has been included in the plot.

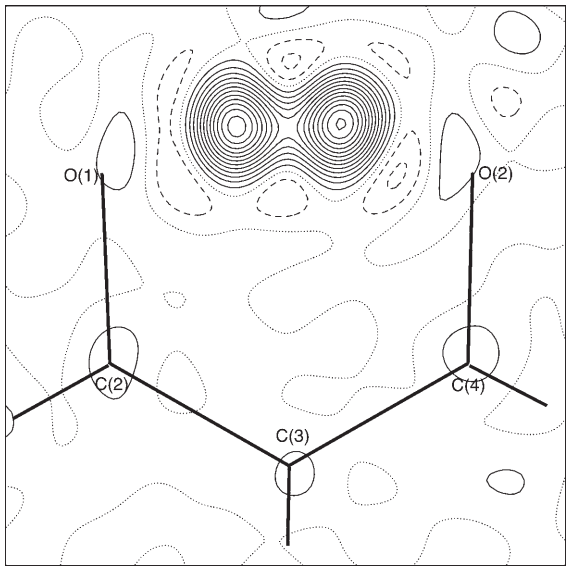

Figure 2. Residual Fourier map from the neutron study with the enol deuteron omitted from the model. The contour interval is 0.05×10^{-14} m Å^{-3}.

Results and Discussion

Neutron diffraction: DBA, see Figure 1, is iso-structural with and very similar to HBA, which was studied previously.[6] A residual Fourier density map from the neutron diffraction study of HBA with the enol hydrogen omitted from the model showed a broad flat hydrogen distribution (Figure 3 of reference [6]). This can be compared with Figure 2 of the present paper, which illustrates the same section for a residual Fourier density map of DBA. The omitted deuteron shows up as a bimodal probability density distribution. Refinement of two deuteron positions leads to two localised positions with bond lengths close to typical O–D distances (Table 1). The deuterium occupancies refined to 0.43(5) for position D(1), 0.44(5) for position D(2), and 0.90(5) for position D(3) indicate a high degree of deuteration (see Figure 1 for labelling of atoms). The MSD of the enol deuteron refine to much smaller values than were found for the enol hydrogen atom in HBA. For comparison the thermal ellipsoid with the positional and thermal parameters obtained for the enol hydrogen in HBA[6] has been included in Figure 1.

We interpret the difference between the HBA and DBA residual Fourier density maps as a clear indication of BA being a case of LBHB with the hydrogen atom vibrating freely between the two oxygen positions and a deuteron tunnelling between two positions, although one could think of arguments against this interpretation. We will rule them out consequently.

Firstly, one might contest that a diffraction study provides direct information that allows us to discriminate dynamic disorder, such as tunnelling between the two positions, from

Table 1. Selected interatomic distances [Å] and angles [°] for deuterated benzoylacetone. For comparison the bond distances found for hydrogenated benzoylacetone[6] are also given.

	DBA, neutron	DBA, X-ray	HBA, neutron
O(1)-O(2)	2.522(2)	2.5219(9)	2.502(4)
O(1)-D(1)	1.002(5)	1.0021(6)	1.329(11)
O(1)-D(2)	1.646(4)	1.6459(6)	
O(2)-D(2)	0.980(4)	0.9771(6)	1.245(11)
O(2)-D(1)	1.611(5)	1.6095(6)	
O(1)-C(2)	1.290(2)	1.2884(8)	1.286(4)
O(2)-C(4)	1.293(2)	1.2940(7)	1.293(4)
C(2)-C(3)	1.403(2)	1.4058(6)	1.414(4)
C(3)-C(4)	1.403(2)	1.4045(6)	1.405(4)
C(1)-C(2)	1.493(2)	1.4958(7)	1.499(4)
C(4)-C(5)	1.482(2)	1.4809(5)	1.483(4)
O(1)-D(1)-O(2)	148.8(4)	149.0(1)	152.3(6)
O(1)-D(2)-O(2)	147.9(4)	147.0(1)	152.3(6)
C(2)-O(1)-D(1)	106.7(3)	106.7(1)	101.2(4)
C(4)-O(2)-D(2)	108.7(3)	109.3(1)	103.2(4)
O(1)-C(2)-C(1)	116.8(1)	117.0(1)	117.0(3)
O(1)-C(2)-C(3)	122.4(1)	122.1(1)	122.1(3)
C(1)-C(2)-C(3)	120.8(1)	120.9(1)	120.9(2)
C(2)-C(3)-C(4)	120.3(1)	120.5(1)	119.7(2)
O(2)-C(4)-C(3)	121.2(1)	121.1(1)	120.9(3)
O(2)-C(4)-C(5)	116.0(1)	116.3(1)	116.4(3)
C(3)-C(4)-C(5)	122.8(1)	122.7(1)	122.6(2)
torsion angles			
O(2)-C(4)-C(5)-C(6)	−173.7(2)	−173.6(1)	−173.5(4)
H(1B)-C(1)-C(2)-O(1)	38.4(5)	38.4(1)	38.0(5)
H(1C)-C(1)-C(2)-O(1)	−82.0(7)	−81.8(1)	−81.0(6)

Table 2. Differences in mean square displacement amplitudes along the interatomic vector $\Delta < u^2 >_{A\text{-}B}$. The numbers correspond to the MSDs extracted from analysis of the X-ray data. Numbers marked in bold correspond to bonded atoms. Values are in 10^{-4} Å^2. The grey areas mark the phenyl and keto–enol groups. The standard deviations are of the order 4–5×10^{-4} Å^2.

	C(1)	C(10)	C(9)	C(8)	C(7)	C(6)	C(5)	C(4)	C(3)	C(2)	O(2)
O(1)	12	−13	−12	−14	−6	−6	−17	−14	−1	**19**	−2
O(2)	−5	−5	−4	−5	2	2	−3	**11**	−3	−7	
C(2)	**1**	−4	−5	−8	−4	−5	−12	−6	**−9**		
C(3)	12	−1	0	−1	4	3	−6	**4**			
C(4)	8	1	3	1	2	−2	**−4**				
C(5)	18	**2**	6	4	5	**2**					
C(6)	15	−3	−2	−2	**2**						
C(7)	15	−1	4	**5**							
C(8)	16	0	**1**								
C(9)	12	**−2**									
C(10)	10										

static disorder, in which the deuteron is statistically distributed between two positions in different molecules. However, analysis of the MSDs has successfully been used to detect static disorder.[21] This was done by showing that static disorder will alter MSDs systematically to deviate from values calculated for rigid body vibration in molecular parts that intuitively should be rigid. Table 2 gives the differences in MSD along interatomic vectors, $\Delta\langle \boldsymbol{u}^2 \rangle_{A\text{-}B}$. Values of $\Delta\langle \boldsymbol{u}^2 \rangle_{A\text{-}B}$ significantly above 10×10^{-4} Å^2 imply non-rigidity in the molecular part.[22] Table 2 shows that the methyl group and to some extent the two oxygen atoms deviate from rigid body behaviour. Similar enhanced vibration of the oxygen atoms was also found in a molecular dynamics study of malonaldehyde,[23] which showed that when a hydrogen atom vibrates freely in the potential between two oxygen atoms the main effect on the framework is an oscillating O···O distance.[23] Static disorder with concomitant changes in bond lengths within the keto–enol ring would increase the $\Delta\langle \boldsymbol{u}^2 \rangle_{A\text{-}B}$ much more than observed,[21] so we rule out static disorder.

Secondly, one might point out that the resolution of the present study is higher than that of the HBA study[6] and that perhaps the resolution of the earlier study was too low to resolve two hydrogen positions. We tried including in the refinement of DBA only data up to the same $\sin\theta/\lambda$ limit as in the HBA study[6] for calculation of the difference maps, but were still able to clearly resolve two deuteron positions. Furthermore, evidence that the HBA and DBA structures are truly different can be found by comparing the structural details in Table 1. It is seen that the O···O distance is lengthened from 2.502(4) Å in HBA[6] to 2.522(2) Å in DBA, conforming with previous observations of the Ubbelohde effect for strong double-well potential HBs,[24] while for very strong single-well potential HBs deuteration will shorten the O···O distance, because the lower ZPVE leads to a more localised deuteron distribution.[25]

X-ray diffraction: We have also measured 11(1) K X-ray data on DBA and there is a very good agreement between the heavy atom positions found in the X-ray and the neutron study (Table 1). This means that the lengthening of the O···O distance from 2.502(4) Å in HBA[6] to 2.522(2) in DBA can be used as indirect evidence of a LBHB.

Obtaining direct information about the hydrogen distribution would require differentiating between the difference charge density of HBA (Figure 9c of reference [16]) and that of DBA. Figure 3 shows the difference Fourier map calculated from the observed X-ray structure factors (phased by the model) and the structure factors calculated for an independent atom model not including the enol deuterons. This map gives a qualitatively quite similar picture to that of HBA[26] and no evident indication of a different distribution of charge in the HBA and DBA molecules.

Ab initio calculations: To gain further insight into the nature of the potential well of the enol hydrogen atom, we have calculated the total energy with respect to constrained hydrogen positions, as described in the computational procedure. The resulting total energies are shown in Figure 4. The three points marked are: MS, corresponding to the minimum energy structure with the hydrogen located on the methyl side; PS, corresponding to the minimum energy structure with the hydrogen located on the phenyl side and

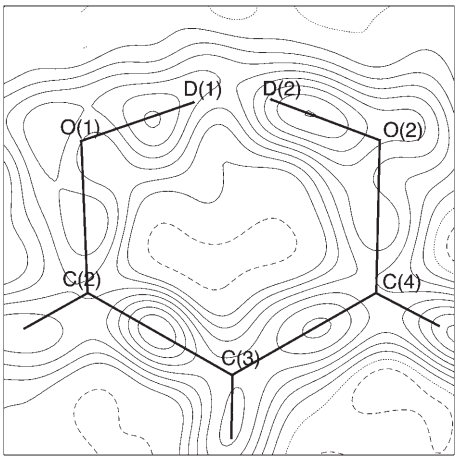

Figure 3. Difference Fourier map calculated from the observed X-ray structure factors and the structure factors calculated for an independent atom model not including the enol deuterons. The contour interval is 0.1 e Å^{-3}.

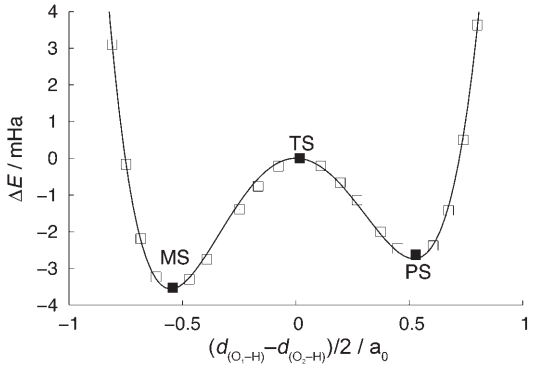

Figure 4. Calculated total energies as a function of the reaction coordinate in bohr radii. The full line corresponds to a fit to a sixth order polynomial. The black points for PS (phenyl side) and MS (methyl side) mark the fully geometry-optimised structures and TS the transition state structure.

TS, the transition state structure. The MS is 3.5 mHa and the PS is 2.6 mHa lower in energy than TS (Table 3). The energies are shown as a function of a reaction coordinate given as: $(d_{(O_1-H)}-d_{(O_2-H)}/2$. Thereby the two energy minima are approximately 0.5 Å apart, as found experimentally (Figures 1 and 2) and theoretically (Table 3).

Table 3. Theoretically calculated atomic distances and energies (E) relative to the TS structure.

	E [mHa]	O(1)−H(Å)	O(2)−H(Å)	O(1)···O(2)(Å)
TS	0.00	1.20	1.21	2.36
MS	−3.5	1.01	1.58	2.51
PS	−2.6	1.56	1.01	2.50

The optimised structures agree well with experiment. The energy differences find the MS to be slightly more stable than the PS, in slight disagreement with the experimental probability density distribution. However, the calculations are on BA in the gas phase, which might not be an optimal model of BA in the crystal. We performed calculations with the torsion angles between the keto–enol group and the methyl and phenyl groups fixed at the experimental values listed in Table 1. This reduced the energy difference between the two sides from 0.9 to 0.5 mHa. A further source of uncertainty is that the B3LYP functional is known to underestimate proton-transfer barriers.[27] The influence of the applied theoretical method could be studied, but, as has just been shown, the results would again be too dependent on small details of the structure and crystal environment for comparisons with experiment to be meaningful at this level of detail. Furthermore, the hydrogen/deuterium atom of course does not reside in a one particle potential, and its motion will be coupled to the rest of the molecule. A full theoretical comparison would thus involve a treatment of all atoms and the crystal environment including anharmonic and quantum effects such as tunnelling[28–30] and lies far beyond the scope of the present work.

The important point is that the calculations show that the potential well is strongly anharmonic and, as will be seen in the following paragraph, BA is exactly in the range of energies over which an effect such as the one observed can be expected. To illustrate the influence of the potential on the eigenstates we have constructed six potential wells, Figure 5, and solved the anharmonic eigenvalue problem as described in the computational section. All six potentials have two minima and are similar to the calculated potential. They differ only by small perturbations, but we will show how these small perturbations can have a large influence on the calculated distribution functions.

In the first potential (Figure 5a), the minima are 1 au (0.529 Å) apart and 3.5 mHa deep. This leads to a clear double maximum in the probability distribution function (φ^2) for the lowest deuterium eigenstate and a clear tunnelling splitting. The lower mass of the proton means that the states lie higher in the potential well, but the lowest state is still below the barrier and consequently a double maximum is also seen in the corresponding hydrogen distribution function. These results are qualitatively comparable to what has been found theoretically by path integral techniques for acetylacetone. Acetylacetone has a weaker hydrogen bond ($d_{O\cdots O}=2.55$ Å) and hence a larger barrier, but both hydrogen and a deuteron are found to tunnel between the two minima.[28] In Figure 5b the minima are only 2 mHa deep, but still 1 au apart. Here the deuteron probability function still shows a double maximum, while the lowest hydrogen state lies at the barrier, and consequently the probability function shows one broad maximum. In Figure 5c we have added a very small linear asymmetric term (given as 0.1 mHa/au$\times x$, which raises the right hand side 0.05 mHa and lowers the left hand side 0.05 mHa) to the potential. This leads to an asymmetric double peak in the deuteron probability distribution and an asymmetric broad single maximum in the proton distribution. This situation is similar to what we have observed for HBA/DBA in which the potential as seen by the proton was an effective single-well po-

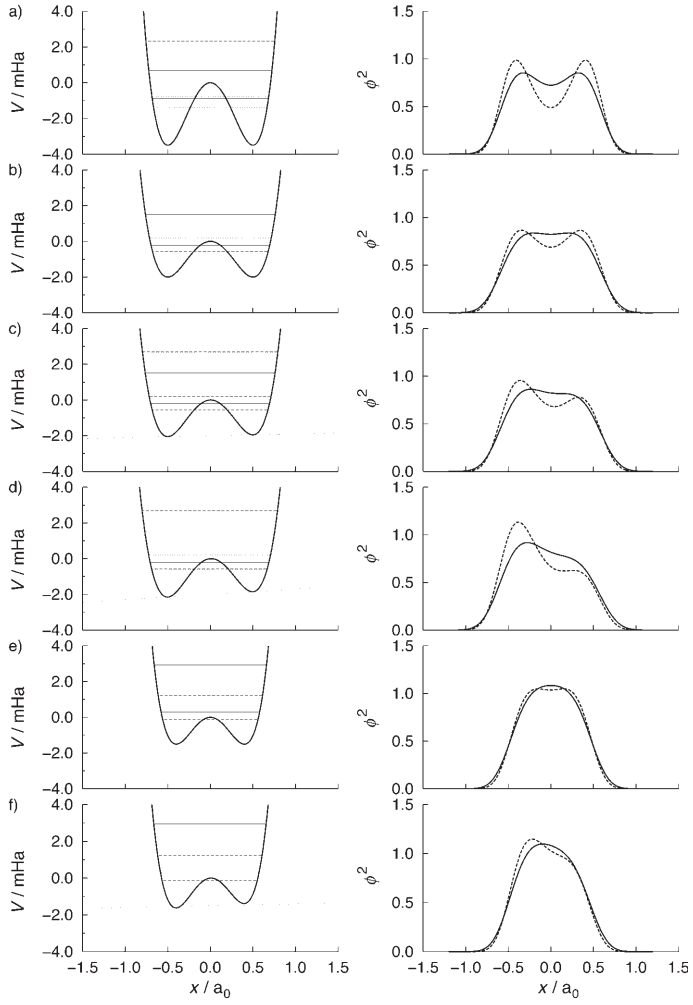

Figure 5. Double-well potentials and their resulting zero point probability distribution functions. The full lines represent hydrogen and the dashed lines deuteron vibrational levels and probability distribution functions. See text for the details of a)–f). The thin dotted lines added to c), d) and f) represent the asymmetric terms added to the potentials.

tential,[6] while for the deuteron we observed a double peak. If a larger asymmetric term (0.3 mHa/au $\times x$) is added (Figure 5d), the proton distribution maintains its broad asymmetric single maximum character, while the deuteron distribution is peaked at one side of the potential. This situation can be compared to what was observed for the Ni–AMBO. In the normal protonated complex the non-hydrogen atoms of the Ni-AMBO conform closely to C_{2v} symmetry, but even so the enol proton was found to be located at a slightly asymmetric position with O–H bond lengths of 1.187(5) and 1.242(5) Å and an O···O distance of 2.420(3) Å.[19] The thermal displacement of the enol hydrogen atom along the O···O direction is substantially bigger than in other directions, which leads to the conclusion that the hydrogen atom moves in a broad single-minimum potential. The deuterated complex showed an even more pronounced asymmetry with O–D bond lengths of 1.058(9) and 1.391(10) Å.[20] However, it is difficult to say anything conclusive as the experiments were performed at room temperature. The tunnel splitting of approximately 1 mHa (Figure 5d) means that the second level, which has a mirror plane and a maximum at the right hand side, will be significantly populated at room temperature. The Ni–AMBO complex would thus be an interesting candidate for a multi-temperature neutron diffraction study. This approach demonstrated its usefulness in explaining the migrating proton by the fact that the two lowest eigenstates of the asymmetric single-well vibrational Hamiltonian are located in opposite sides of the potential well.[15] As the temperature is lowered the second level will be depopulated, the average position of the proton will shift and the proton migrates as a function of temperature.[15]

Finally we have constructed two potentials in which the minima are just 0.8 Bohr apart and 2 mHa deep (Figure 5e and 5f). In Figure 5f we have furthermore added the same small asymmetric term as in Figure 5c. In both cases the lowest energy levels lie at the barrier and the potentials are effectively single-well potentials. We believe the symmetric case has recently been observed by neutron diffraction for the very short hydrogen bond in the molecule 4-cyano-2,2,6,6-tetramethyl-3,5-heptanedione (CTMH).[31] The compound CTMH is claimed to have the shortest symmetrical O–H···O hydrogen bond yet reported with $d_{O\cdots O}$ = 2.388(5) Å.[31] Neutron crystallography (20 K data) revealed the hydrogen-bonded proton to be nearly centred (O–H = 1.216(9) Å and O···H = 1.220(8) Å) between the two oxygen atoms. In the slightly asymmetric case (Figure 5f) the probability distribution is shifted markedly and it is clear that even a small perturbation can result in a relatively large change in the mean hydrogen/proton position. Such a situation we recently observed in nitromalonamide (NMA),[32] which offers another example of an equally very short O–H···O hydrogen bond at an O···O distance of 2.391(3) Å.[32] Neutron crystallography (15 K data) showed that the enol hydrogen atom had an asymmetric position, due to intermolecular hydrogen bonding, O–H = 1.140(10) Å and H···O = 1.308(11) Å, between the two oxygen atoms in the otherwise quite symmetrical molecule.

Discussion: Steiner and Saenger have compiled much information on the geometry of O–H···O hydrogen bonds from a survey of low-temperature neutron diffraction studies.[33] Based on results from 81 low-temperature neutron diffraction structures, they showed that there is a smooth correlation between O–H and H···O distances in O–H···O interactions. An interpolated curve through these data points is shown in Figure 6. The O–H bond continuously elongates with concomitant shortening of the H···O distance until a symmetric O–H···O geometry is reached at an O···O separation of about 2.39 Å.

We have superimposed on the curve results from the present study of deuterated benzoylacetone as well as for the previously studied normal benzoylacetone,[6] and also results from the Ni–AMBO studies.[19,20] It is worth noting that for both the Ni–AMBO and BA, the deuterated samples show distances in good accordance with the Steiner and Saenger curve. In contrast to this, the normal protonated BA and

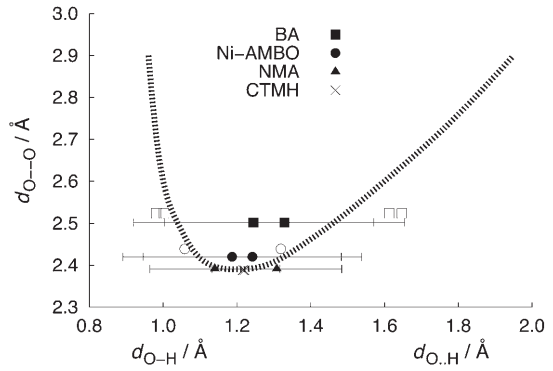

Figure 6. Interpolated curve using the data of Steiner and Saenger.[33] The structures of nitromalonamide[32] (NMA), benzoylacetone[6] (BA), the cyano-tetramethyl-heptanedione (CMTH) and Ni-AMBO[19,20] have been superimposed. The horizontal lines indicate the size of the root mean square displacement of the enol hydrogen along the O···O vector. The filled points correspond to the hydrogenated samples and the open points to the deuterated samples.

Ni–AMBO structures show O–H distances that are intermediate between values at the two branches of the Steiner–Saenger curve (see Figure 6). However, this can be reconciled by viewing the proton as shuttling freely between two positions in a broad shallow potential well. In a standard crystallographic refinement the width of the potential well is measured by the root-mean-square displacement (RMSD). In a standard harmonic model the RMSD is the half-width of the Gaussian probability density distribution.[34]

The RMSD component of the O–H···O hydrogen atom along the O···O direction is also marked in Figure 6. For the Ni–AMBO the RMSD of hydrogen in the O···O direction is 0.37 Å at room temperature and for HBA the RMSD of hydrogen along the O···O direction is 0.28 Å at 20 K. In the study of protonated BA this leads to the conclusion that the hydrogen atom moves in a broad single-minimum potential. With the added information from the present study of the deuterated compound one may conclude in greater detail that the potential should be described as a weakly asymmetric (almost symmetric) low-barrier potential, similar to Figure 5c. The deuterium atom tunnels between two possible localised positions and the enol proton even at the low temperature of 15 K has sufficient energy to shuttle over the low-energy barrier.

We have also superimposed on the Steiner–Saenger curve data from the very short hydrogen bonds in CTMH[27] and NMA.[28] The bond lengths show good agreement with the curve. It is interesting to note that in both systems the thermal motion of the enol hydrogen atom is much elongated along the direction between the two oxygen atoms.[35] In NMA the RMSD of the enol hydrogen atom along the O···O vector is 0.18 Å at 15 K.[22] The RMSD is also shown in Figure 6 and the enol hydrogen atom makes substantial excursions in a broad potential around the midpoint[36] between the two oxygen atoms and the hydrogen vibrates freely in what can be considered an effective single-well potential.

The large RMSD of the enol hydrogen raises the question of how the structure of a short strong hydrogen bond should be described. At the heart of a correlation such as the Steiner–Saenger curve presented in Figure 6 lies a view of a structure as a set of coordinates/interatomic distances. However, the fact that the enol hydrogen atom has an RMSD larger than the difference in hydrogen-bonded distances shows that summarizing the structure of a short hydrogen-bonded system just by a hydrogen coordinate is too simplistic a model. We did put forward a similar view in the study of NMA.[32] Here the mean position (coordinate) of the hydrogen was found significantly closer to one oxygen atom than the other. However, the calculated probability density function for the enol hydrogen atom showed that there is also a large probability of finding the enol hydrogen atom close to the other oxygen atom.[32]

Gilli et al. recently presented an attempt of a general description of the nature of the strong O–H···O hydrogen bond in β-diketone enol RAHB systems.[37] They illustrated the possible shapes of hydrogen-transfer potentials, ranging from symmetric single wells with barriers of different heights, to weakly asymmetric single wells, to asymmetric double wells with different barrier heights. Gilli et al. proceeded to present a few 100 K X-ray structures of compounds with hydrogen bonds of the internal RAHB keto–enol type and used them to illustrate the variety in nature of the strong O–H···O hydrogen bond. They also referred to our work on HBA,[6] and suggested that the intramolecular hydrogen bond has a weakly asymmetric double-well low-barrier potential. We arrive at the same conclusion for the qualitative shape of the potential well. However, there is a big difference in the interpretation of the resulting hydrogen bond. Gilli et al. suggested that the hydrogen bond in BA is disordered, a static distribution of tautomeric forms.[37] We have ruled out static disorder on the basis of the Hirshfeld rigid-bond test and instead, by detailed analysis of ab initio calculations, shown that the very low temperature neutron diffraction data can be explained by a deuterium atom tunnelling between two possible localised positions and an enol proton that, even at the low temperature of 15 K, has sufficient energy to shuttle over the low-energy barrier.

The conclusion of Gilli et al. that the hydrogen bond in BA is disordered, a static distribution of tautomeric forms,[37] was based on the result of their so-called λ-test which relies on a correlation between the π-delocalisation and a proton-transfer reaction coordinate. Several structures do not fit these correlations and were claimed to give "incorrect" positions in the correlation diagrams because of internal structural disorder due to double-well hydrogen bonds being misinterpreted as single-well hydrogen bonds.[37] Among the so-called "mispositioned points" was our low-temperature neutron and X-ray diffraction study of HBA.[6] In our opinion the methodologies, and hence conclusions by Gilli, are problematic for a number of reasons. First of all, we find a procedure in which a correlation is postulated, and many results that do not agree with the expected behaviour are simply claimed to be "mispositioned"

without further justification, to be problematic. Secondly, if a correlation between the hydrogen position and the symmetry of the ring is to be claimed it should be based on only high quality data. The correlations given and the analysis of the hydrogen-transfer pathways in the work by Gilli et al. is largely based on 38 selected putative accurate crystal structures mostly determined from X-ray data collected at room temperature. This was done in spite of the well-known problem of carrying out an accurate deconvolution of positional and thermal parameters solely from analysis of X-ray data, in particular for the hydrogen atoms. The severe asphericity problem in the charge density accumulating in the covalent O–H bond creates an artificial shortening of the O–H bond, which is not properly addressed. As discussed above there is very little difference between the difference charge density of HBA (Figure 9c by Herbstein et al. in reference [26]) and that of DBA, Figure 3. They look very much the same although the hydrogen-transfer pathways in the two cases are very different. We agree that Gilli et al. earlier demonstrated a certain correlation between the O···O distance and the symmetry of the enol ring.[5] However, the correlation between the ring symmetry and the hydrogen position is much more controversial in our opinion. Firstly there are the above-mentioned reservations, whether one can meaningfully speak of a hydrogen coordinate in a short hydrogen bond. Secondly, the flat potential well means that the hydrogen can be shifted significantly in the hydrogen bond with little change of the energy of the system. As an example the hydrogen-bond energy in NMA was more than 110 kJ mol^{-1}, while the difference in energy between centred and off-centred hydrogen was only 0.3 kJ mol^{-1} (0.1 mHa).[32] Consequently the enol hydrogen position can easily be perturbed. This is seen both experimentally, in which intermolecular hydrogen bonding leads to an asymmetric hydrogen position,[32] and theoretically, in which the addition of a small asymmetry term to the model potential leads to a large shift in mean position (Figure 5f). Experimentally it was also found that an asymmetric hydrogen position resulted in only a small deviation from symmetry in the enol ring. NMA was not included in the correlations by Gilli.[37]

Conclusion

We have shown how an enol deuteron in benzoylacetone has a bimodal probability density function, while an enol hydrogen atom was earlier shown to have a broad unimodal probability density function. This is the very definition of a low-barrier hydrogen bond. By analysis of very low temperature neutron diffraction data supported by extensive theoretical calculations, we have shown how the data can be interpreted as the deuterium atom tunnelling between two possible localised positions and the enol proton having sufficient energy to shuttle over the low-energy barrier, even at 15 K.

We have thereby underlined the dynamic and quantum nature of the hydrogen bond. The zero-point probability distributions of the hydrogen positions in short O···O hydrogen bonds corresponding to selected double-well potentials have been calculated (Figure 5), and show the diversity and rich detail in the nature of the strong O···O hydrogen bonds. Structure correlation studies such as the ones reported in references [3,5,14,33,37] are definitely useful in getting an overview of hydrogen-bonded systems, but also risk oversimplifying a problem that is, in its nature, complex. Figures 5 and 6 underline the inherent dynamic nature of the hydrogen bond and that the hydrogen position can not be described fully by a single coordinate. Neutron diffraction studies of individual cases will continue to be very desirable in efforts to obtain more general understanding of chemical bond aspects of the O–H···O hydrogen bond.

Experimental Section

Sample preparation: Benzoylacetone was deuterated by repeated recrystallisation in CH_3OD. This readily exchanges H with D for the enol hydrogen atom between O(1) and O(2) and the H at C(3). As the signal from the keto–enol hydrogen is difficult to detect by NMR spectroscopy, the degree of deuteration was monitored by the peak corresponding to the hydrogen bound to C(3). Large single crystals were grown by slow evaporation of CH_3OD containing a seed crystal.

Neutron diffraction: Single-crystal neutron diffraction data were collected at 15 ± 0.5 K by using monochromatic thermal neutrons with a wavelength of 0.955 Å on D19, a four-circle neutron diffractometer, on the H11 thermal beam at the Institut Laue-Langevin, Grenoble. A structural model including anisotropic thermal parameters on all atoms was fitted to the experimental data. The relevant experimental and refinement details are summarised in Table 4.

Table 4. Experimental details for deuterated benzoylacetone.

	X-ray study	Neutron study
formula	$C_{10}O_2H_8D_2$	$C_{10}O_2H_8D_2$
space group	$P2_1/c$	$P2_1/c$
a [Å]	8.016(1)	8.015(1)
b [Å]	5.486(1)	5.485(1)
c [Å]	19.445(3)	19.462(1)
β [°]	110.37(1)	110.34(1)
V [Å^3]	801.6(2)	802.2(1)
λ [Å]	0.5616	0.840
T [K]	11(1)	15(1)
data collection		
diffractometer	type 512 HUBER	D19 at the ILL
scan method	ω-2θ	normal beam Weissenberg
measured reflns	21063	4536
unique reflns	6613	3388
R_1	2.90%	5.10%
index range	$-7 \le h \le 15$	$-12 \le h \le 12$
	$-10 \le k \le 10$	$0 \le k \le 9$
	$-38 \le l \le 24$	$0 \le l \le 30$
refinement		
$R(F)/R(F^2)$ [%]	2.85/3.94	7.60/9.83
$wR(F)/wR(F^2)$ [%]	2.78/5.46	8.04/14.23
GoF	0.978	2.340
observed reflns [$I > 2\sigma(I)$]	4644	2921
parameters	393	209
weighting scheme	$1/\sigma^2(F^2)$	$1/\sigma^2(F^2)$

X-ray diffraction: Single-crystal X-ray diffraction data were collected at 11 ± 0.5 K using $Ag_{K\alpha}$ radiation on a four-circle diffractometer with a displex mounted. A full multipole model[38] including a functional expansion up to the octapole level for the carbon and oxygen atoms and up to the quadrupole level for the hydrogen atoms was used. The hydrogen atoms were fixed at the positions found in the neutron study. MSDs for the hydrogen atoms were derived by scaling the values obtained in the neutron study. The relevant experimental and refinement details are summarised in Table 4.

Ab initio calculation: All calculations were carried out using a density functional theory approach applying the hybrid functional B3LYP[39,40] in combination with Dunning's correlation consistent triple-zeta basis set, cc-pVTZ[41] as implemented in Gaussian 03.[42] All calculations were done using the ultrafine integration grid for calculation of the two-electron integrals. The transition state was localised by using the keyword TS in the optimisation. The potential-energy curve was constructed by means of an internal reaction coordinate (IRC keyword) calculation in combination with relaxed potential-energy surface scans from the two minima. The IRC was initiated from the transition-state structure and stepping three steps in each direction. From the two local minima, the curve was extrapolated by scanning the two distances, $d_{(O_1-H)}$ and $d_{(O_2-H)}$, in increments of ± 0.025 Å. Towards the transition state of the PES, two structures were computed from each minimum, whereas four additional structures were found for compression of the two O–H covalent bonds.

For solving the anharmonic vibrational Hamiltonian we used a method similar to the one we used for the rattling heavy atom in clathrates.[43] An anharmonic Hamiltonian corresponding to a one particle potential is constructed from a suitably chosen reference harmonic Hamiltonian. The matrix elements of the Hamiltonian on the harmonic basis functions then have simple expressions and a direct diagonalisation gives the anharmonic eigenstates and eigenenergies. Our approach differs somewhat from an earlier study[15] as it is not perturbative, and consequently potentials with several minima and resulting tunnelling can be treated, as long as the basis functions are carefully chosen.[43]

Acknowledgements

The help of Allesandra Silvani in deuterating benzoylacetone is gratefully acknowledged. Computation time was allocated by the Danish Center for Scientific Computing. B.S. thanks the Natural Danish Science Research Council for a Skou grant. G.K.H.M. thanks the Carlsberg Foundation for financial support.

[1] F. Hibbert, J. Emsley, *Adv. Phys. Org. Chem.* **1990**, 26, 255–379.
[2] G. A. Jeffrey, *An introduction to Hydrogen Bonding*, Oxford University Press, **1997**.
[3] T. Steiner, *Angew. Chem.* **2002**,*114*, 50–80; *Angew. Chem. Int. Ed.* **2002**, *41*, 48–76.
[4] W. W. Cleland, *Biochemistry* **1992**, *31*, 317–319.
[5] P. Gilli, V. Bertolasi, V. Ferretti, G. Gilli, *J. Am. Chem. Soc.* **1994**, *116*, 909–915.
[6] G. K. H. Madsen, B. B. Iversen, F. K. Larsen, M. Kapon, G. M. Reisner, F. H. Herbstein, *J. Am. Chem. Soc.* **1998**, *120*, 10040–10045.
[7] C. Flensburg, S. Larsen, R. F. Stewart, *J. Phys. Chem.* **1995**, *99*, 10130–10141.
[8] a) W. W. Cleland, M. M. Krevoy, *Science* **1994**, *264*, 1887–1890; b) P. A. Frey, S. A. Whitt, J. B. Tobin, *Science* **1994**, *264*, 1927–1930; c) A. Warshel, A. Papazyan, P. A. Kollman, W. W. Cleland, M. M. Kreevoy, P. A. Frey, *Science* **1995**, *269*, 102–106.
[9] P. A. Frey, *J. Phys. Org. Chem.* **2004**, *17*, 511–520.
[10] C. N. Schutz, A. Warshel, *Proteins: Struct., Funct., Bioinf.* **2004**, *55*, 711–723.
[11] C. N. Fuhrmann, M. D. Daugherty, D. A. Agard, *J. Am. Chem. Soc.* **2006**, *128*, 9086–9102.
[12] a) M. Benoit, D. Marx, M. Parrinello, *Nature* **1998**, *392*, 258–261; b) M. Benoit, D. Marx, *ChemPhysChem* **2005**, 6, 1738–1741.
[13] C. C. Wilson, *Acta Crystallogr. Sect. B* **2001**, *57*, 435–439.
[14] C. A. Morrison, M. M. Siddick, P. J. Camp, C. C. Wilson, *J. Am. Chem. Soc.* **2005**, *127*, 4042–4048.
[15] F. Fontaine-Vive, M. R. Johnson, G. J. Kearley, J. A. K. Howard, S. F. Parker, *J. Am. Chem. Soc.* **2006**, *128*, 2963–2969.
[16] T. Steiner, I. Marjerz, C. C. Wilson, *Angew. Chem.* **2001**, *113*, 2728–2731; *Angew. Chem. Int. Ed.* **2001**, *40*, 2651–2654.
[17] J. A. Cowan, J. A. K. Howard, G. J. McIntyre, S. M.-F. Lo, I. D. Williams, *Acta Crystallogr. Sect. B* **2003**, *59*, 794–801.
[18] J. A. Cowan, J. A. K. Howard, G. J. McIntyre, S. M.-F. Lo, I. D. Williams, *Acta Crystallogr. Sect. B* **2005**, *61*, 724–730.
[19] E. O. Schlemper, W. C. Hamilton, S. T. La Placa, *J. Chem. Phys.* **1971**, *54*, 3990–4000.
[20] B. Hsu, E. O. Schlemper, C. K. Fair, *Acta Crystallogr. Sect. B* **1980**, *36*, 1387–1391.
[21] a) J. D. Dunitz, V. Schomaker, K. N. Trueblood, *J. Phys. Chem.* **1988**, *92*, 856–867; b) J. D. Dunitz, E. F. Maverick, K. N. Trueblood, *Angew. Chem.* **1988**, *100*, 910–926; *Angew. Chem. Int. Ed. Engl.* **1988**, *27*, 880–895.
[22] F. L. Hirshfeld, *Acta Crystallogr. Sect. A* **1976**, *32*, 239–244.
[23] K. Wolf, W. Mikenda, E. Nusterer, K. Schwarz, C. Ulbricht, *Chem. Eur. J.* **1998**, *4*, 1418–1427.
[24] M. Ichikawa, *Acta Crystallogr. Sect. B* **1978**, *34*, 2074–2080.
[25] F. Takusagawa, T. F. Koetzle, *Acta Crystallogr. Sect. B* **1979**, *35*, 2126–2135.
[26] F. H. Herbstein, B. B. Iversen, M. Kapon, F. K. Larsen, G. K. H. Madsen, G. M. Reisner, *Acta Crystallogr. Sect. B* **1999**, *55*, 767–787.
[27] V. Barone, C. Adamo, *J. Chem. Phys.* **1996**, *105*, 11007–11019.
[28] K. Hinsen, B. Roux, *J. Chem. Phys.* **1997**, *106*, 3567–3577.
[29] M. E. Tuckerman, D. Marx, *Phys. Rev. Lett.* **2001**, *86*, 4946–4949.
[30] R. Iftime, J. Schofield, *J. Chem. Phys.* **2001**, *114*, 6763–6773.
[31] J. A. Belot, J. Clark, J. A. Cowan, G. S. Harbison, A. I. Kolesnikov, Y.-S. Kye, A. J. Schultz, C. Silvernail, X. Zhao, *J. Phys. Chem. B* **2004**, *108*, 6922–6926.
[32] G. K. H. Madsen, C. Wilson, T. M. Nymand, G. J. McIntyre, F. K. Larsen, *J. Phys. Chem. A* **1999**, *103*, 8684–8690.
[33] T. Steiner, W. Saenger, *Acta Crystallogr. Sect. B* **1994**, *50*, 348–357.
[34] B. T. M. Willis, A. W. Pryor, *Thermal Vibrations in Crystallography*, Cambridge University Press, **1975**.
[35] This is seen from the plot of the thermal ellipsoids in CTMH. Unfortunately the MSD of the hydrogen are not included in the attached structure in reference [31] Therefore we can not study it quantitatively.
[36] It should also be pointed out that the RMSD is actually a small number compared to the distances covered by the enol hydrogen. To just cover 50% of the probability density distribution a distance of 1.54 times the RMSD is needed.
[37] P. Gilli, V. Bertolasi, L. Pretto, V. Feretti, G. Gilli, *J. Am. Chem. Soc.* **2004**, *126*, 3845–3855.
[38] T. Koritsanszky, S. Howard, P. R. Mallinson, Z. Su, T. Richter, N. K. Hansen, XD, a computer program package for multipole refinement and analysis of charge densities from diffraction data, Institute of Crystallography, Freie Universität, Berlin, **1995**.
[39] A. D. Becke, *J. Chem. Phys.* **1993**, *98*, 5648–5652.
[40] C. Lee, W. Yang, R. G. Parr, *Phys. Rev. B* **1988**, *37*, 785–789.
[41] T. H. Dunning, Jr., *J. Chem. Phys.* **1989**, *90*,1007–1023.
[42] Gaussian 03, Revision B.05, M. J. Frisch, G. W. Trucks, H. B. Schlegel, G. E. Scuseria, M. A. Robb, J. R. Cheeseman, J. A. Montgomery, Jr., T. Vreven, K. N. Kudin, J. C. Burant, J. M. Millam, S. S. Iyengar, J. Tomasi, V. Barone, B. Mennucci, M. Cossi, G. Scalmani, N. Rega, G. A. Petersson, H. Nakatsuji, M. Hada, M. Ehara, K. Toyota, R. Fukuda, J. Hasegawa, M. Ishida, T. Nakajima, Y. Honda, O. Kitao, H. Nakai, M. Klene, X. Li, J. E. Knox, H. P. Hratchian, J. B. Cross, V. Bakken, C. Adamo, J. Jaramillo, R. Gomperts, R. E. Stratmann, O. Yazyev, A. J. Austin, R. Cammi, C. Pomelli, J. W. Ochterski, P. Y. Ayala, K. Morokuma, G. A. Voth, P. Salvador, J. J. Dannenberg, V. G. Zakrzewski, S. Dapprich, A. D. Daniels, M. C.

Strain, O. Farkas, D. K. Malick, A. D. Rabuck, K. Raghavachari, J. B. Foresman, J. V. Ortiz, Q. Cui, A. G. Baboul, S. Clifford, J. Cioslowski, B. B. Stefanov, G. Liu, A. Liashenko, P. Piskorz, I. Komaromi, R. L. Martin, D. J. Fox, T. Keith, M. A. Al-Laham, C. Y. Peng, A. Nanayakkara, M. Challacombe, P. M. W. Gill, B. Johnson, W. Chen, M. W. Wong, C. Gonzalez, J. A. Pople, Gaussian, Inc., Wallingford CT, **2004**.

[43] G. K. H. Madsen, G. Santi, *Phys. Rev. B* **2005** *72*, 220301(R.

Received: October 19, 2006
Published online: March 15, 2007

